Laser Physics Letters



LETTER

# Hybrid fiber laser integrating fast and slow active media for accurate synthesis of high-energy arbitrary optical waveforms by cavity dumping



Laser Phys. Lett. **19** (2022) 075104 (8pp) https://doi.org/10.1088/1612-202X/ac6b44

Letter

# Hybrid fiber laser integrating fast and slow active media for accurate synthesis of high-energy arbitrary optical waveforms by cavity dumping

**Boris Nyushkov**[1,2,*], **Aleksey Ivanenko**[1] **and Sergey Smirnov**[1]

[1] Novosibirsk State University, 630090 Novosibirsk, Russia
[2] Novosibirsk State Technical University, 630073 Novosibirsk, Russia

E-mail: b.nyushkov@nsu.ru

Received 13 February 2022
Accepted for publication 25 April 2022
Published 31 May 2022

**Abstract**
We demonstrate the possibility of the accurate direct laser synthesis of high-energy arbitrary optical waveforms by the programmable driving of partial cavity dumping in a specific continuous-wave fiber laser. To this effect we have developed an original hybrid laser configuration which integrates two different active media. The first medium, a semiconductor optical amplifier (SOA), acts as a saturated lumped preamplifier. It features a relatively fast (sub-nanosecond) gain recovery, and thus effectively suppresses the intracavity power fluctuations induced by cavity dumping. The second active medium, an erbium-doped fiber amplifier (EDFA), acts mainly as a booster amplifier. This distributed inertial amplifying medium effectively accumulates pump energy, thereby providing an enhancement of output energy upon cavity dumping. Our simple proof-of-concept laser setup has allowed the synthesis of nanosecond arbitrary optical waveforms with an energy up to 40 nJ and arbitrarily tunable repetition rate. The proposed combination of a slow (EDFA) and fast (SOA) amplifying stages prevents the laser from strong relaxation oscillations and power flux fluctuations which essentially restrict cavity dumping in conventional rare-earth-doped fiber lasers. The applied two-stage intracavity spectral filtering ensures spectral purity of a rather narrowband ($\leqslant$0.1 nm) laser output. For the purpose considered, the integrated SOA-EDFA laser configuration is preferable to a conventional architecture 'master oscillator—power amplifier' whose nonlinear gain can obstruct the accurate synthesis of high-energy optical waveforms.

Keywords: fiber laser, fiber amplifier, semiconductor optical amplifier, cavity dumping, optical waveforms

(Some figures may appear in colour only in the online journal)

* Author to whom any correspondence should be addressed.

 

## 1. Introduction

The generation of coherent arbitrary optical waveforms is of great practical interest and drives continued research into different methods and techniques of electronically-controllable pulse shaping in laser sources, or the external synthetization of waveforms from pulsed laser radiation. Among the most advanced external approaches are those which rely on wavelength-division or time-division manipulation with subsequent multiplexing of an optical frequency comb, or an ultrashort pulse train. These were originally referred to as 'Fourier-domain pulse shaping' [1] and 'temporal coherence synthetization' [2], respectively. Despite their essentially high temporal resolution, these methods feature an inherent experimental complexity in their implementation. They usually require producing a coherent optical frequency comb (or un ultrashort pulse train) and precisely-controllable arrays of devices for frequency or time-domain manipulation of the radiation [3–5]. This motivates the continued search for alternative, simpler and cheaper solutions for the generation of coherent arbitrary optical waveforms. Thus, in last decade, prominent research has been dedicated to the development of direct versatile control over pulse shaping in mode-locked fiber lasers. This well-established and quite affordable type of laser features a unique design flexibility and excellent performance in terms of energy efficiency, beam quality, and noise. Various intracavity methods for the manipulation of pulse shaping (by means of in-cavity spectral and phase shapers) were proposed for passively [6–10] and actively mode-locked fiber lasers [11, 12]. However, studies of pulse shaping capabilities of those methods were limited to a few shapes. The methods requires complicated in-cavity devices for the manipulation of spectral amplitudes or/and phases. Some of those methods have yet to be realized experimentally. Moreover, most of the proposed methods do not allow for the scaling up of radiation power (energy), since they can be affected by enhanced optical nonlinearity in the fiber cavity. The only high-power solution [9] relies on a sophisticated digital micromirror device incorporated into a large-mode-area photonic crystal fiber laser cavity which cannot be considered either as a reliable or an affordable choice. Its capability to shape arbitrary waveforms (in terms of the temporal profile) was not explored in full. Therefore, novel, more reliable and affordable, practical methods for the programmable production of high-energy arbitrary waveforms by means of fiber laser sources is still in demand.

Recently, we presented an original configuration of an actively mode-locked fiber laser which employs a semiconductor optical amplifier (SOA) as an active medium, and a waveguide electro-optic switch (WEOS) as a variable output coupler [13]. It was shown that certain modulation of the WEOS-based output coupling in the fast gain recovery configuration can drive either a high-quality active mode locking, or cavity dumping with pulsed output of almost the same quality. The 'partial' cavity dumping explored in such a laser configuration allowed wide-range (multi-octave) continuous tuning of the repetition rate of the output pulses, and their arbitrary programmable shaping [14]. This regime was referred to as 'partial' cavity dumping, since it is based on the repeatable partial switching of the laser output coupling from total intracavity confinement of laser radiation towards its total extraction. The allowable degree of such partial switching is determined mainly by the following necessary conditions: continuous operation above the lasing threshold and a monotonous increase of the laser output power with increasing the output coupling. Such a cavity-dumped operation of the aforementioned SOA-based laser configuration was free from relaxation oscillations which are inherent in the case of rare-earth-doped fiber lasers, and restrict the possible timing of cavity dumping [15]. However, conventional SOA cannot store as much energy as the fiber-based active media like the erbium-doped fiber amplifier (EDFA). Therefore, cavity dumping of the solely-SOA-based configuration yields a low-energy ($\sim$1 nJ at most) pulsed output on the nanosecond time scale [13]. At the same time, the possible use of an external EDFA is not an optimal way to facilitate the accurate synthesis of high-energy optical waveforms, because of the nonlinear dependence of the gain on the instantaneous input power [16, 17], which may distort waveforms featuring large amplitude variations. Another drawback of an external EDFA in the context of the accurate synthesis of high-energy optical waveforms is the contribution of amplified spontaneous emission, which rises with increase of the time intervals between the waveforms. To solve those issues, we have developed and present herein a novel, integrated SOA-EDFA-based laser configuration for the accurate direct synthesis of high-energy arbitrary optical waveforms by programmable cavity dumping. The SOA serves as a saturated preamplifier for the intracavity EDFA (used as a power booster) and thus prevents the laser from relaxation oscillations upon partial cavity dumping through the WEOS. The laser sustains narrowband continuous-wave (cw) lasing, which remains almost unaffected, even under partial cavity dumping. Such an approach has been demonstrated in our proof-of-concept laser setup for the first time and has allowed the synthesis of arbitrary optical waveforms with nanosecond duration and energy of up to 40 nJ at an arbitrarily tunable repetition rate. The method allows for the further scaling up of waveform energy as well as for further improvement of its temporal resolution.

## 2. Experimental setup

A schematic diagram of the studied laser system is shown in figure 1. For explanation of the concept, it is supplemented with insets which qualitatively map intracavity and extracavity variation of the lasing power in the explored regime of partial cavity dumping. The laser has a ring fiber cavity with a WEOS-based variable output coupler and three 1:99 reference couplers (RC1…RC3). While the WEOS forms the main laser output, the reference couplers serve for monitoring the intracavity power distribution. The laser employs two amplifying media, namely a fiber-coupled SOA (Thorlabs SOA 1013S) and an EDFA. The latter consists of a 1.4 m long

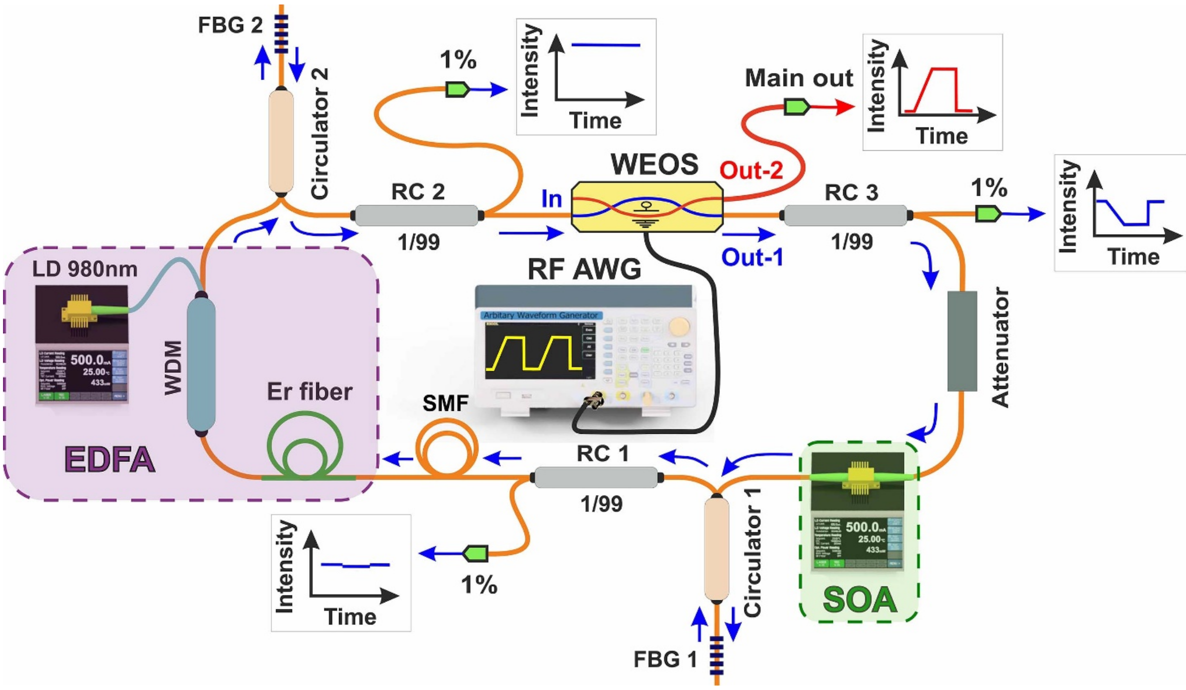


**Figure 1.** Schematic diagram of the studied laser system: SOA—semiconductor optical amplifier, RC1…RC3—reference couplers, WEOS—a waveguide electro-optic switch, SMF—single-mode fiber, FBG 1, FBG 2—fiber Bragg gratings, EDFA—erbium-doped fiber amplifier. the insets illustrate the character of lasing power variation induced by partial cavity dumping in different parts of the laser system.

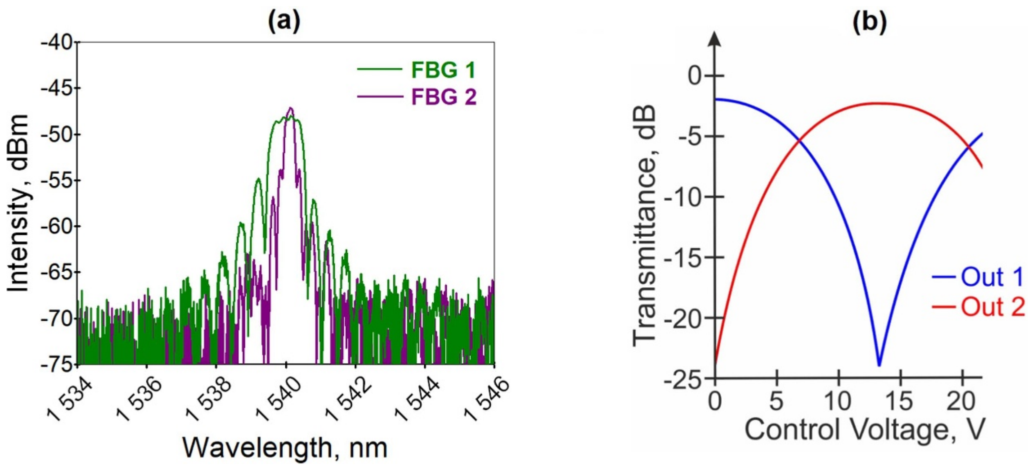


**Figure 2.** (a) Measured reflection spectra of the FBG 1 (green curve) and the FBG 2 (violet curve). (b) Typical optical transmission of the WEOS to the intracavity output port 1 (blue curve) and to the extra-cavity output port 2 (red curve) versus the control voltage (according to the WEOS spec for monochromatic light at 1550 nm).

erbium-doped fiber (Liekki Er30-4/125) and a wavelength-division multiplexor which enables the injection of pumping radiation at 980 nm. The pump source is a laser diode with a constant power of ~500 mW. Each amplification stage is followed by narrowband bandpass filters composed of a fiber-optic circulator and a fiber Bragg grating (FBG). The grating reflection spectra are centered at ~1540 nm. They are as narrow as ~1 nm (FBG 1) and ~0.3 nm (FBG 2). Their reflection spectra (measured with a resolution of 0.02 nm) are shown in figure 2(a). Their bandwidth difference ensures tolerance to a possible slight mismatch between their central wavelengths. The FBGs prevent broadband multi-wavelength lasing, which might emerge in lasers with such active media [18], and ensure the spectral purity of the resulting narrow-band laser output. The circulators enforce unidirectional lasing in the cavity. The cavity contains also a delay line-inset of a 200 m long single-mode fiber. It is used to extend the intracavity round-trip time ($T_{RT}$) for laser radiation to nearly 1 microsecond. Such a long round-trip time is chosen to prevent possible distortions of the outputted nanosecond waveforms due to a possibly incomplete recovery of the intracavity cw radiation during its one round trip. The extended round-trip time fulfills the condition of the fast recovery gain: $T_{\mathrm{recovery}} \ll T_{\mathrm{RT}}$. The SOA is pumped electrically in the constant-current regime (at 500 mA) and can provide a saturable gain varying from 18.7 dB (small signal gain) towards a unity gain (achievable with a signal power of ~17 dBm). Normally, the SOA operates as the saturated preamplifier in this laser. Its input power and saturation are roughly adjusted by installing an appropriate optical attenuator at the SOA input. It also protects the SOA from excessive input signal power. The next amplification stage, namely the booster EDFA, scales up the cw intracavity power delivered to the voltage-controlled WEOS-based output coupler. Programmable dynamic control of this coupler allows for the dumping of desirable optical waveforms. A commercial four-port polarization independent $LiNbO_3$ electrooptic switch (EOSpace SW-2×2-PI-SFU-SFU-UL) is employed as such an output coupler. It provides gradually variable cross-coupling between the input and output ports, as illustrated in figure 2(b). The zero-voltage state of the WEOS corresponds to the lowest output coupling (−24 dB) and to the lowest intracavity loss. Raising the control voltage up to 12.5 V results in the gradual switching of the WEOS optical transmission to the extra-cavity output port, thereby increasing the laser output coupling and intracavity loss. The inherent permanent insertion loss of the WEOS is about 2.4 dB. The switching time of the used WEOS is about 10 ns. The electrical control signal is synthesized by means of a programmable radiofrequency arbitrary waveform generator (RF AWG, Rigol DG4162).

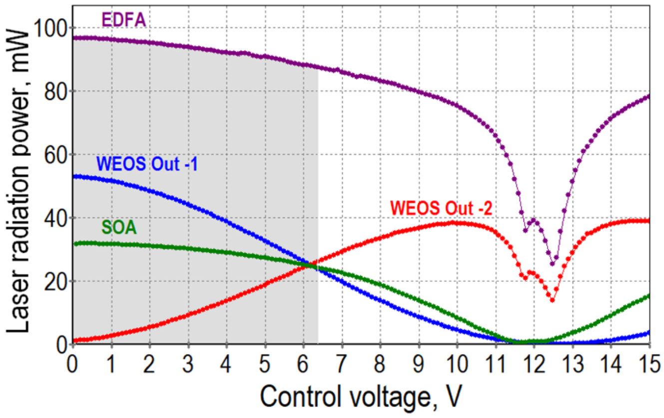


**Figure 3.** Intracavity and output power characteristics of the cw lasing governed by the WEOS control voltage: the intracavity laser power delivered to the EDFA input by the SOA stage (green curve), the intracavity laser power delivered to the WEOS input by the EDFA stage (violet curve), the output laser power extracted from the WEOS output port 2 (red curve), and the residual intracavity laser power monitored at the WEOS intracavity output port 1 (blue curve). The shaded area corresponds to an optimal voltage sweep for waveform production by partial cavity dumping. Within the indicated voltage range the intracavity laser power sustained at the WEOS input port remains rather saturated (varies by less than 10%).

## 3. Results and discussion

First, we studied the dependence of cw lasing on varied cross-coupling between the ports of the WEOS incorporated into the laser cavity. To this effect, we applied the direct-current control voltage to the WEOS. While varying this voltage, we measured the resulting laser radiation power independently at the WEOS extra-cavity output port 2 and at the extra-cavity ports of the 1:99 reference couplers. The latter allowed deriving the intracavity laser power sustained at the WEOS intracavity input port and the residual intracavity power after radiation dumping via the WEOS. Figure 3 summarizes the obtained power characteristics. These characteristics were acquired over the voltage range of the univocal response of the WEOS (0–12.5 V), and thus the whole available range of the cross-coupling variation (~22 dB according to the WEOS spec) was explored.

The measured power characteristics testify to a multiple increase in lasing power as compared with the solely-SOA-based laser configurations [13, 14], due to incorporation of the additional EDFA stage into the cavity. They also suggest that partial cavity dumping will not dramatically affect the sustained cw lasing regime. Indeed, if the output coupling is manipulated by the WEOS control voltage variation within the range 0–6.3 V, it will lead to a moderate variation (of less than 10%) of the lasing power delivered to the WEOS input by the EDFA stage (as indicated by the violet curve in figure 3). At the same time, the WEOS-based output coupling and the WEOS-inserted intracavity loss will vary much more significantly (from −24 dB to −7 dB and from −2.4 dB to −5 dB, respectively) as seen in figure 2(b). In spite of such variations, the proposed laser configuration sustains cw lasing almost unaffected integrally, due to the compensation of the WEOS-induced drops in intracavity power by the deeply saturated SOA stage with fast gain recovery. This minimizes the fluctuation of the intracavity lasing power delivered to the EDFA stage. The EDFA stage also features some degree of saturation. It delivers finally boosted and flattened (over time) lasing power to the WEOS input.

Thus, the proposed configuration can, in principle, provide fast (one-round-trip) recovery of the lasing power upon short-term (as compared with the round-trip time) partial cavity dumping. The sub-nanosecond recovery time of the SOA gain ensures that such partial cavity dumping will not be accompanied by relaxation oscillations originated from the SOA itself if the dumping is developed on the nanosecond (or longer) time scale [13, 14]. Moreover, the SOA stabilizes the lasing power at the EDFA input, and thus prevents the slow relaxation oscillations which are typical for the solely-EDFA-based cavity-dumped laser configurations [15].

An optimal voltage sweep for the accurate synthesis of arbitrary optical waveforms by cavity dumping has to satisfy the requirements of monotony and linearity of the laser output response. Our study of waveform synthesis was conducted mainly by exploiting the control voltage range of 0–6.3 V, which limits the maximal output peak power to 25 mW. However, one can also exploit the extended range (0–10 V) in order to provide a higher peak power (up to 40 mW) of the synthesized optical waveforms at the cost of their slight distortion. Thus, the WEOS-based output coupling can reach almost −3 dB.

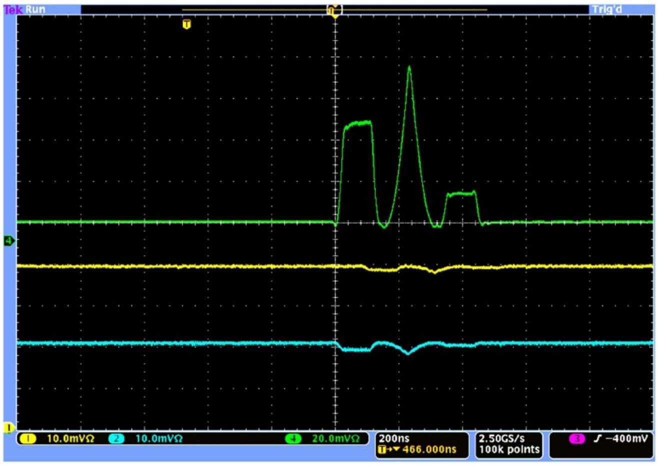


**Figure 4.** An oscilloscope screenshot with the simultaneously acquired time traces of the optical waveform outputted through the WEOS (upper trace) and the residual intracavity laser power variation (lower traces) monitored via the reference couplers. The time scale is 200 ns per division.

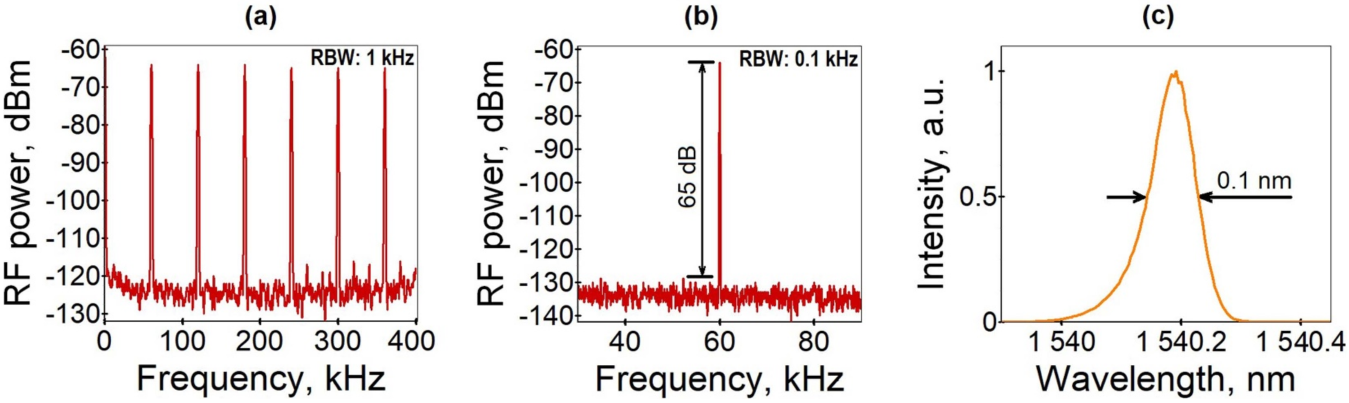


**Figure 5.** Radiofrequency (a), (b) and optical (c) spectra of a regular train of the above optical waveforms (figure 4) produced by partial cavity dumping at the 60 kHz repetition rate. RBW—resolution bandwidth of the RF analyzer.

Based on the above description, we switched the laser operation over partial cavity dumping driven by arbitrary radiofrequency waveforms synthesized, by means of the programmable RF AWG. An example of the resulting laser synthesis of optical waveforms is shown in figure 4. This figure represents an oscilloscope screenshot with synchronous time traces of the optical waveform produced by partial cavity dumping (upper trace) and the residual intracavity laser power variation (lower traces), monitored via the reference fiber couplers. The oscillogram testifies to the relatively accurate transfer of the trapezoid-triangle-trapezoid profile of the control electric signal to the time-intensity profile of the optical waveform. The waveform duration (at $-10$ dB level) was about 440 ns and its repetition rate was initially set at 60 kHz. It is seen also that the intracavity cw power flux is maintained steady (being weakly affected by cavity dumping) owing to the combined action of the saturated amplification stages.

Shown in figures 5(a) and (b) are the radiofrequency spectra of a regular train of the above optical waveforms measured with different resolutions. These spectra feature a relatively high signal-to-noise ratio which exceeds 60 dB at the waveform repetition frequency (figure 5(b)). There is no appearance of any parasitic beats and phase-noise pedestals within the measured frequency spans. This testifies to the high reproducibility and low time jitter of the optical waveforms in the train. Figure 5(c) represents a measured optical spectrum of the obtained optical waveform train. The spectrum width at half maximum is as narrow as about 0.1 nm (with allowance for the measurement resolution of 0.02 nm).

The repetition rate of the optical waveform synthesis can be widely and continuously tuned, since the cw lasing power at the WEOS input remains stable upon partial cavity dumping. The upper limit for this tuning is imposed by the waveform duration and the WEOS response time. We have examined synthesis of the above-described optical waveform not only at kHz but also at MHz scale repetition rates. Figure 6 represents the measured time trace of a regular train of the above optical waveform produced by partial cavity dumping at the 1 MHz repetition rate (red trace). Synchronous monitoring of the intracavity laser power variation, via the reference couplers, has revealed that dumping-induced drops in the instantaneous intracavity power (after the WEOS) are compensated for

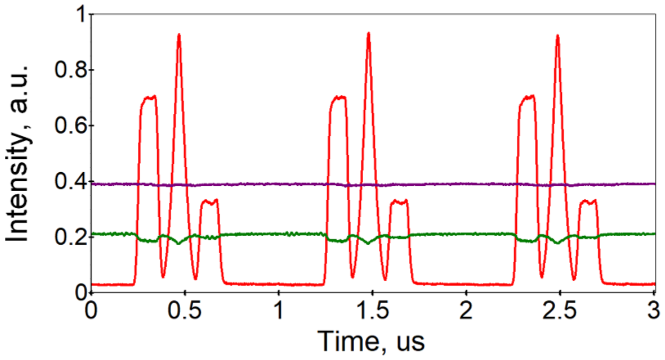


**Figure 6.** Measured time traces of a regular train of the above optical waveforms produced by partial cavity dumping at the 1 MHz repetition rate (red trace) and residual intracavity laser power variation (green and violet traces) simultaneously monitored via the reference couplers.

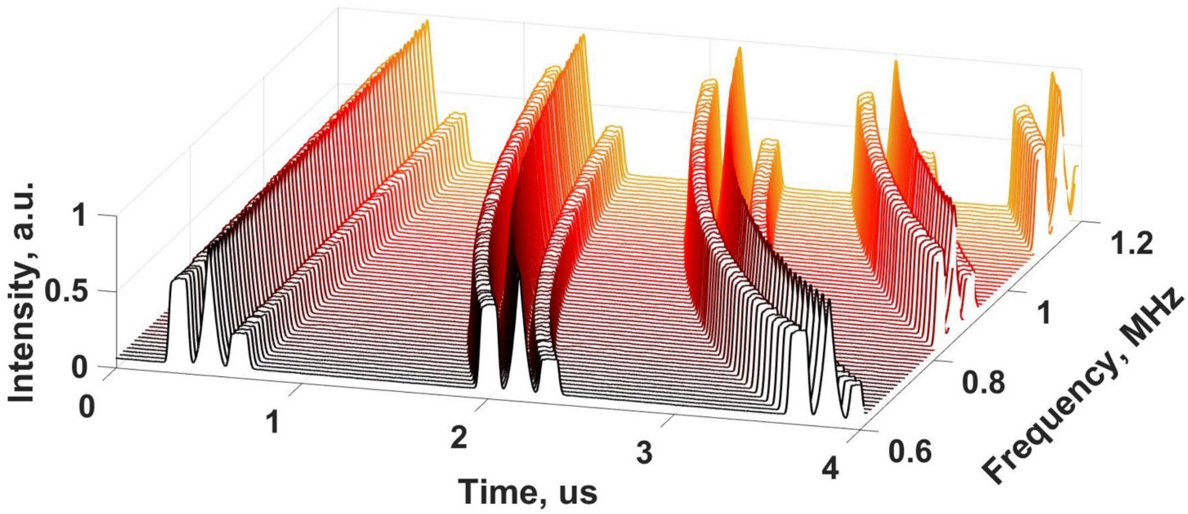


**Figure 7.** Time traces of the optical waveform train measured at the repetition rate being swept from 0.6 to 1.2 MHz.

during passing through the both amplification stages. Thus, the WEOS input is always fed with a nearly constant cw lasing power, even upon partial cavity dumping (as testified to by the violet trace in figure 6).

Figure 7 proves the possibility of wide-range (octave-spanning) continuous tuning of the optical waveform repetition rate, without affecting its time-intensity profile. Here demonstrated are time traces measured sequentially at the different repetition rates ranging from 0.6 MHz to 1.2 MHz.

The measured radiofrequency spectra of the optical waveform train with the 1 MHz repetition rate also feature a relatively high signal-to-noise ratio, as seen in figures 8(a) and (b). This feature, along with the absence of apparent parasitic beats and phase-noise pedestals, testifies to the high reproducibility and low time jitter of the optical waveforms in the train. The optical spectrum turned out to be almost unaffected by switching the waveform repetition rate from kHz to MHz (figure 8(c)). Thus, the overall quality of the optical waveform synthesis at the kHz and MHz repetition rates is similarly high.

The maximum achievable repetition rate of optical waveform synthesis was limited to 40 MHz, mainly by the programmable RF AWG used, which can synthesize a nanosecond control electric signal with the required voltage at such a maximum repetition rate. The next limiting factor is a finite modulation bandwidth of the WEOS itself. We believe however that with faster equipment it will be possible to explore sub-GHz repetition rates in the proposed laser configuration. The most advanced commercial $LiNbO_3$-based WEOS are known to be nearly as fast as congener waveguide electro-optic intensity modulators.

The energy of a synthesized optical waveform is governed by its power-time profile. The described laser configuration can provide an output peak power of up to 40 mW as seen in figure 3. Thus, the energy can approach 40 nJ in an optical waveform synthesized over the whole nanosecond time scale. This exceeds the energy achievable in the solely-SOA-based laser configurations [13, 14] by almost one order of magnitude. The obtainable energy is comparable with that of the solely-EDFA-based cavity-dumped laser reported in [15] which, however, does not allow the accurate arbitrary shaping of the output laser pulses and wide-range continuous tuning of their repetition rate, in contrast to our laser configuration. We believe that the energy characteristics of our configuration can

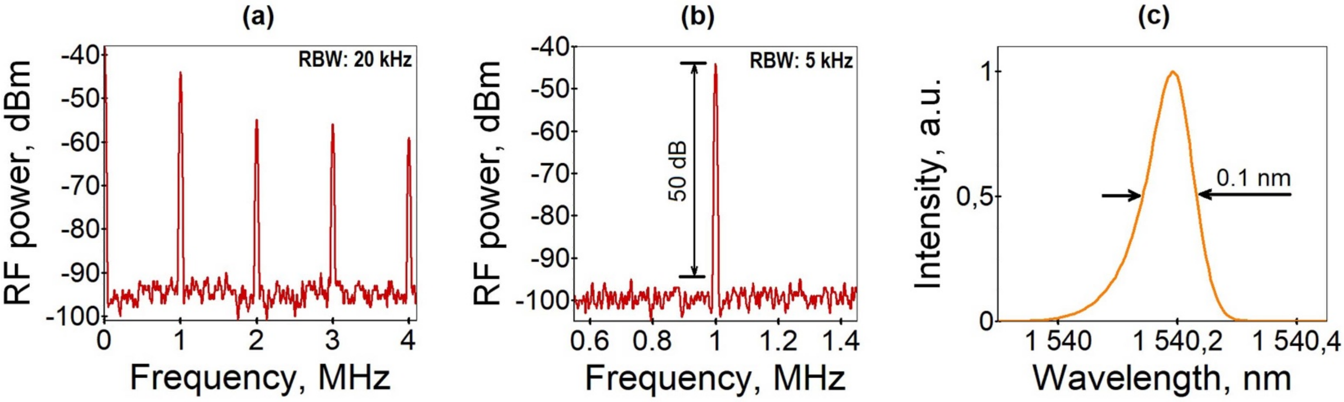


**Figure 8.** Radiofrequency (a), (b) and optical (c) spectra of a regular train of the above optical waveforms (figure 6) produced by partial cavity dumping at the 1 MHz repetition rate. RBW—resolution bandwidth of the RF analyzer.

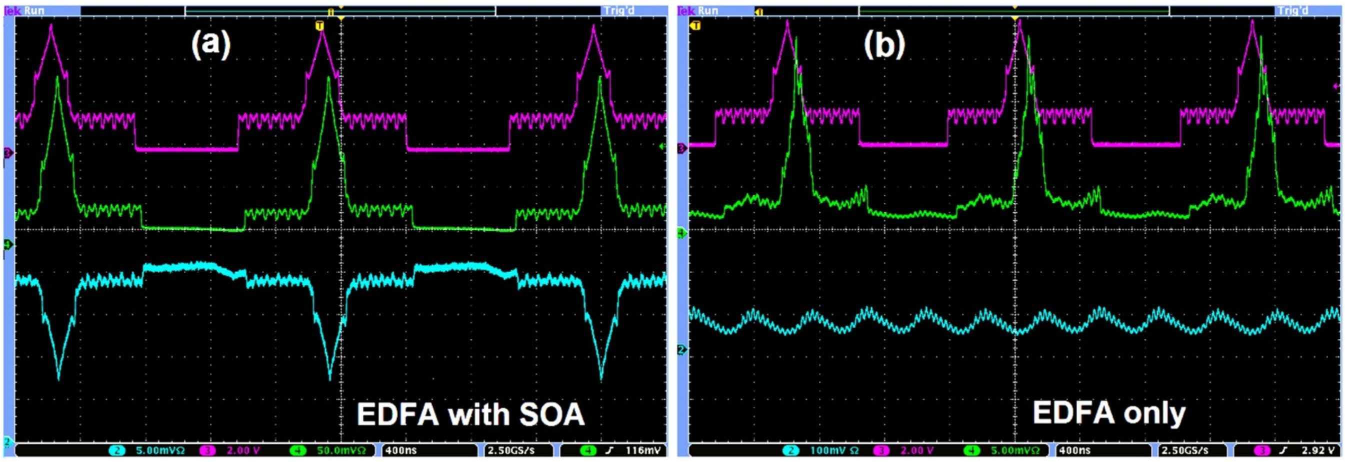


**Figure 9.** Oscilloscope screenshots with simultaneously measured time traces of the control electric signal (upper trace), the corresponding optical waveform outputted through the WEOS (middle trace), and the residual intracavity laser power variation (lower trace) monitored via the reference couplers: (a) the measurement performed with the original laser configuration, which employs both the SOA and EDFA; (b) the measurement performed after removal of the SOA from the original laser configuration. The amplitudes of the control electric signals are the same. The time scales are 400 ns per division.

be further enhanced by applying a more powerful intracavity EDFA, as well as by the fine optimization of the input power and the saturation degree for each amplification stage in the laser.

It is worth noting that the demonstrated possibility of the accurate synthesis of high-energy arbitrary optical waveforms is provided mainly by the unique combination of two different amplification stages in the laser. The deeply saturated low-inertia SOA stage prevents possible relaxation oscillations and parasitic fluctuations of the intracavity power flux, while the EDFA stage boosts the output energy characteristics of the laser. Figure 9 represents measured time traces that additionally corroborate this thesis. The integrated SOA-EDFA laser configuration allows the synthesis of even sophisticated optical waveforms via cavity dumping as seen in figure 9(a). However, after removal of the SOA stage from the laser, its cavity-dumped operation becomes affected by the parasitic fluctuations of intracavity power flux, and therefore does not allow the same accurate synthesis of optical waveforms as seen in figure 9(b). When making a comparison, one should also allow for some difference in the output power characteristics of the SOA-EDFA and pure-EDFA laser configurations. The same variation of the WEOS control voltage in these configurations led to different (even in magnitude) variations of output laser power. This factor, along with occurrence of high-amplitude parasitic oscillations affecting the intracavity power flux in the pure-EDFA laser configuration, made it necessary to apply different sensitivity settings for the oscillogram measurements, as seen in the bottom bars in figures 9(a) and (b). Nevertheless, intracavity power flux was evidently affected by the strong parasitic oscillations, with characteristic times correlating with temporal features of the control electric signal in the pure-EDFA laser configuration only (figure 9(b)). Therefore, this configuration did not allow for obtaining such accurate optical waveforms as those produced by the integrated SOA-EDFA laser configuration (figure 9(a)).

## 4. Conclusion

Thus, we have proposed and proved experimentally an original method for the accurate laser synthesis of high-energy arbitrary optical waveforms. The method is based on the programmable driving of partial cavity dumping in a fiber laser which integrates a fast and slow active media, namely SOA and EDFA. The deeply saturated low-inertia SOA stage prevents possible relaxation oscillations and parasitic fluctuations of intracavity power flux, while the EDFA stage boosts the output energy characteristics of the laser.

The presented approach has a number of distinguishing features related both to its underlying physics and usability. In particular, stationary narrowband cw lasing in the developed laser configuration remains effectively unaffected, in spite of repeatable partial cavity dumping. This allows for the accurate synthesis of rather coherent arbitrary optical waveforms with an almost arbitrarily tunable pulse repetition rate. This is a quite affordable technique which is easy-to-implement and easy-to-use as compared with other methods, for instance, with those based on Fourier-domain pulse shaping. As a proof of concept, we have implemented an experimental setup which allows the synthesis of arbitrary optical waveforms with a few ns resolution, energy up to 40 nJ, and a spectral bandwidth of about 0.1 nm. Relying upon the current state of the art in waveguide optical switches, EDFAs and waveguide filters, we believe that time resolution, energy characteristics and spectral purity of the reported method can yet be significantly improved.

The reported method of accurate laser synthesis of high-energy arbitrary optical waveforms with arbitrarily tunable repetition rate may find application in various lidar measurements (remote sensing) and tasks related to specific nonlinear light-matter interactions.

## Acknowledgment

This work was supported by the Russian Science Foundation (Grant No. 17-72-30006).

## Conflict of interest

The authors declare no conflicts of interest.

## ORCID iDs

Boris Nyushkov https://orcid.org/0000-0002-3913-1230
Aleksey Ivanenko https://orcid.org/0000-0002-6331-6067
Sergey Smirnov https://orcid.org/0000-0002-4137-600X

## References

[1] Weiner A M 1995 Femtosecond optical pulse shaping and processing *Prog. Quantum Electron.* **19** 161–237
[2] Park Y, Asghari M H, Ahn T-J and Azaña J 2007 Transform-limited picosecond pulse shaping based on temporal coherence synthesization *Opt. Express* **15** 9584–99
[3] Scott R P, Fontaine N K, Heritage J P and Yoo S J B 2010 Dynamic optical arbitrary waveform generation and measurement *Opt. Express* **18** 18655–70
[4] Liao J, Wen H, Zheng X, Zhang H and Zhou B 2012 A time-domain photonic arbitrary waveform generator *Opt. Express* **20** 12631–9
[5] Wu D S, Richardson D J and Slavík R 2015 Optical Fourier synthesis of high-repetition-rate pulses *Optica* **2** 18–26
[6] Boscolo S, Finot C, Karakuzu H and Petropoulos P 2014 Pulse shaping in mode-locked fiber lasers by in-cavity spectral filter *Opt. Lett.* **39** 438–41
[7] Peng J and Boscolo S 2016 Filter-based dispersion-managed versatile ultrafast fibre laser *Sci. Rep.* **6** 25995
[8] Iegorov R, Teamir T, Makey G and Ilday F Ö 2016 Direct control of mode-locking states of a fiber laser *Optica* **3** 1312–5
[9] Liu W, Fan J, Xie C, Song Y, Gu C, Chai L, Wang C and Hu M 2017 Programmable controlled mode-locked fiber laser using a digital micromirror device *Opt. Lett.* **42** 1923–6
[10] Karar A S, Ghandour R, Mahariq I, Alboon S A, Maaz I, Neji B and Barakat J M H 2020 A programmable mode-locked fiber laser using phase-only pulse shaping and the genetic algorithm *Photonics* **7** 69
[11] Nakazawa M and Hirooka T 2016 Mode locking theory of the Nyquist laser *Opt. Express* **24** 4981–95
[12] Nakazawa M and Hirooka T 2021 Theory of AM mode-locking of a laser as an arbitrary optical function generator *IEEE J. Quantum Electron.* **57** 1300320
[13] Nyushkov B, Ivanenko A, Smirnov S, Shtyrina O and Kobtsev S 2020 Triggering of different pulsed regimes in fiber cavity laser by a waveguide electro-optic switch *Opt. Express* **28** 14922–32
[14] Nyushkov B, Kobtsev S, Ivanenko A and Smirnov S 2020 Synthesis of periodic and aperiodic arbitrary waveforms in a SOA-fibre laser *Proc. SPIE* **11547** 115471C
[15] Malmström M, Yu Z, Margulis W, Tarasenko O and Laurell F 2009 All-fiber cavity dumping *Opt. Express* **17** 17596–602
[16] Shtyrina O V, Ivanenko A V, Yarutkina I A, Kemmer A V, Skidin A S, Kobtsev S M and Fedoruk M P 2017 Experimental measurement and analytical estimation of the signal gain in an Er-doped fiber *J. Opt. Soc. Am.* B **34** 227–31
[17] Shtyrina O, Kokhanovskiy A, Yarutkina I, Skidin A, Ivanenko A, Efremov S, Nyushkov B, Smirnov S and Fedoruk M 2020 Study of gain efficiency in quasi-distributed amplification systems *Opt. Lett.* **45** 499–502
[18] Zhang Z, Wu J, Xu K, Hong X and Lin J 2009 Tunable multiwavelength SOA fiber laser with ultra-narrow wavelength spacing based on nonlinear polarization rotation *Opt. Express* **17** 17200–5